Modeling effect of cover condition and soil type on rotavirus transport in surface flow

Rabin Bhattarai, Paul C. Davidson, Prasanta K. Kalita and Mark S. Kuhlenschmidt

ABSTRACT

Runoff from animal production facilities contains various microbial pathogens which pose a health hazard to both humans and animals. Rotavirus is a frequently detected pathogen in agricultural runoff and the leading cause of death among children around the world. Diarrheal infection caused by rotavirus causes more than two million hospitalizations and death of more than 500,000 children every year. Very little information is available on the environmental factors governing rotavirus transport in surface runoff. The objective of this study is to model rotavirus transport in overland flow and to compare the model results with experimental observations. A physically based model, which incorporates the transport of infective rotavirus particles in both liquid (suspension or free-floating) and solid phase (adsorbed to soil particles), has been used in this study. Comparison of the model results with experimental results showed that the model could reproduce the recovery kinetics satisfactorily but under-predicted the virus recovery in a few cases when multiple peaks were observed during experiments. Similarly, the calibrated model had a good agreement between observed and modeled total virus recovery. The model may prove to be a promising tool for developing effective management practices for controlling microbial pathogens in surface runoff.

Key words | contamination, hydrology, pathogen, water quality

Rabin Bhattarai (corresponding author)
Paul C. Davidson
Prasanta K. Kalita
Department of Agricultural and Biological Engineering,
University of Illinois,
1304 W. Pennsylvania Avenue,
Urbana,
IL 61801,
USA
E-mail: *rbhatta2@illinois.edu*

Mark S. Kuhlenschmidt
Department of Pathobiology,
University of Illinois,
2001 S. Lincoln Avenue,
Urbana,
IL 61802,
USA

INTRODUCTION

Nearly all animal housing facilities such as feedlots, barns, and pens are believed to be primary sources of microbial contamination of surface water resources. Microbial pathogens present in agricultural runoff impose a significant risk to health when acquired directly via the fecal-oral route or indirectly as a waterborne contaminant. As per Waterborne Disease and Outbreak Surveillance System (WBDOSS) of Center for Disease Control and Prevention (CDC), there have been 794 waterborne disease outbreaks causing more than 575,000 illnesses from 1971 to 2006 in the United States (Bhattarai 2011). Furthermore, rotavirus is a leading cause of death of children around the globe. Rotavirus infection kills more than 500,000 children under the age of five every year, most of them in developing countries (Feng *et al.* 2002). Even in a developed country like the United States, rotavirus was estimated to be the cause of about 60,000 hospitalizations and 37 deaths annually during 1993–2003 (Fischer *et al.* 2007). Apart from humans, rotavirus has a wide host range including many mammalian species like pigs (Ferrari & Gualandi 1986), lambs (Wray *et al.* 1981), foals (Conner & Darlington 1980), rabbits (Conner *et al.* 1988) and deer (Smith & Tzipori 1979).

The risk of pathogenic contamination is not only a human health hazard but also a potential threat to the continued existence of animal operations. To design and develop pathogen control practices, microbial transport processes in surface runoff need to be properly understood and quantified along with various factors that affect pathogen

doi: 10.2166/wh.2017.240

transmission to the environment. There have been several studies which looked into the transport of pathogens such as *Cryptosporidium* (Harter *et al.* 2000; Atwill *et al.* 2002; Tate *et al.* 2004; Trask *et al.* 2004; Koch *et al.* 2013; McLaughlin *et al.* 2013; Davidson *et al.* 2014) and bacteria (Smith *et al.* 1985; McMurry *et al.* 1998; Gagliardi & Karns 2000; Jamieson *et al.* 2002; Passmore *et al.* 2010). There are very limited studies which have investigated the fate and transport of viruses in soil and water systems (Powelson *et al.* 1990; Sim & Chrysikopoulos 2000; Chu *et al.* 2003; Ojha *et al.* 2011; Davidson *et al.* 2013, 2016; Gotkowitz *et al.* 2016).

It is very time and resource consuming to monitor the influence of multiple environmental factors on pathogen fate and transport. Therefore, modeling can provide a consistent quantitative approach to estimate pathogen loading under a wide range of environmental conditions. In terms of modeling pathogen transport phenomena, there are few studies in the literature that model the transport and fate of pathogens in water flow (Moore *et al.* 1989; Walker *et al.* 1990; Canale *et al.* 1993; Wilkinson *et al.* 1995; Fraser *et al.* 1998; Tian *et al.* 2002; Dorner *et al.* 2006; Parajuli *et al.* 2009; Bhattarai *et al.* 2011; Niazi *et al.* 2015; Liao *et al.* 2016). Pachepsky *et al.* (2006) reviewed the status and challenges in manure-borne pathogen transport modeling in the environment. Similarly, Jamieson *et al.* (2004) reviewed different approaches in microbial transport modeling in surface waters at the watershed scale. A few studies have estimated surface transport of bacteria using simple empirical equations which relate bacteria transport to runoff rate or depth (Moore *et al.* 1989; Fraser *et al.* 1998; Tian *et al.* 2002). However, the empirical transport equations used in these models have not been well tested and validated. The parameters do not have a physical basis and must be obtained through calibration. Surface transport of bacteria in SWAT (Sadeghi & Arnold 2002) and COLI (Walker *et al.* 1990) are computed based on the modified universal soil loss equation which is also an empirical model. As pathogen transport models move from a small laboratory setting to a large scale such as a watershed (Walker & Stedinger 1999; Dorner *et al.* 2006; Parajuli *et al.* 2009), the model prediction uncertainties are enhanced. Very few modeling studies have linked sediment transport to pathogen movement in water (Bhattarai *et al.* 2011; Pandey *et al.* 2016). The objective of this study was to model the fate and transport of infective rotavirus particles in surface flow using a process-based model. The results of this study can help in developing the guidelines for translating the model into practice for designing best management practices (BMPs) such as a vegetative filter strip (VFS). Previous studies have shown the promising potential of VFS in reducing sediment, nutrients, pesticides and pathogens from runoff (Atwill *et al.* 2002; Tate *et al.* 2004; Trask *et al.* 2004; Koch *et al.* 2013; Mclaughlin *et al.* 2013; Davidson *et al.* 2014).

METHODOLOGY

Experimental setup

The rotavirus overland transport experiments were completed using three soils (Catlin silt-loam, Alvin fine sandy-loam, and Darwin silty-clay) and three cover conditions (bare soil, Smooth Brome, and Fescue vegetation) at the University of Illinois. Three soil types used in this study span the range of sand and clay contents for soils typically found in Illinois. The methodology is described in detail in Davidson *et al.* (2016) with a condensed summary included below.

The rainfall simulator used in this study measured 1.07 × 0.66 m in size and was constructed using 12.7 mm PVC pipe. Since adequate droplets were not produced by the mister nozzles, a common fiberglass window screen with 1 mm square openings was placed 305 mm below the arrangement of nozzles. The nozzles sprayed water onto the screen and droplets were allowed to fall onto the surface below, more closely mimicking natural rainfall droplets. This small scale rainfall simulator can produce rainfall intensities from 23 to 90 mm/hr. In this study, 65 mm/hr rainfall intensity, which represents the 25-year event for east-central Illinois, was used for all soil and cover conditions.

Soil bed boxes (0.610 m long by 0.305 m wide by 0.015 m deep) used during experimental studies were made from 6.35 mm thick Plexiglas. A total of 11 holes with 4.76 mm diameter were drilled 76.2 mm above the bottom of the soil box (corresponding to soil surface location) to allow for the collection of surface runoff. The Plexiglas soil boxes were placed in a wooden frame which allowed the slope adjustment of the box frame. Two

aluminum trays were placed on the down-slope end of the wood frame to collect surface flow samples.

Three different soils were collected and placed in the small-scale soil chambers. These soils represent the typical range of soil textures in Illinois. A moderately drained silt-loam (Catlin series: 24% sand, 50% silt, 26% clay) soil was obtained from an agricultural field in Champaign, IL. Similarly, a well-drained fine sandy loam (Alvin series: 60% sand, 25% silt, 15% clay) soil and poorly drained silty-clay (Darwin series: 5% sand, 50% silt, 45% clay) soil were collected from a farm near Newton, IL. Since the soil chambers were designed for 76 mm of soil and soil texture would remain somewhat constant in such a small depth range, the top 76 mm of soil was collected after removing all vegetation and organic material from the soil surface. The soil was oven-dried at 105 °C for 24 hours to reduce existing microbial activity that could interfere with sample analyses and then packed in three one-inch (25.4 mm) layers. Each layer was moistened and compacted with a plate. Rainfall was applied on a regular basis after placing three layers of soils in the chamber to simulate natural compaction. Two vegetation covers used in this study were Smooth Brome and Tall Fescue (purchased at Illini FS, Urbana, IL). The seeding rate for each grass was 16.8 kg/ha. It took approximately 4–6 months to achieve the desired maturity level of vegetation before use in transport studies. The surface runoff samples were collected and analyzed for rotavirus. Surface runoff samples were collected every minute after runoff began.

Extraction and quantification of rotavirus

Group A Porcine rotavirus OSU strain (P9[7], G5) was obtained from the American Type Culture Collection catalog # VR-892 and passaged two additional times in cultured Ma104 cells Three colostrum-deprived newborn piglets were inoculated with 1 mL (3×10^6 FFU) each, and the feces were pooled and collected for 2 days. Rotavirus was prepared by cultivation in Ma104 cells and purified as described by Rolsma *et al.* (1998), excluding the last CsCl gradient step.

Since the collected surface runoff samples contained a relatively high concentration of rotavirus particles, a dilution of the samples was necessary for analysis. A 1/5 dilution was prepared by mixing 200 μL of the sample with 800 μL of serum-free MEM and applying 500 μL directly to the plate wells. Similarly, soil core samples were prepared by combining 250 μL of the sample with 750 μL of serum-free MEM and applying 500 μL to the plate wells.

The focus forming unit (FFU) assay was performed following previously published methods (Rolsma *et al.* 1998). The rotavirus FFUs were enumerated by counting the number of the FFUs present in a given sample at a ×100 magnification using a Nikon TS 100 inverted microscope equipped with a computer-controlled electronic stage and Spot RT-slider CCD camera. The experimental results were used to parameterize and validate the model results.

Modeling framework

The following possible states of virus fate and transport in overland flow were considered based on the stochastic framework proposed by Yeghiazarian *et al.* (2006) and modified from the process-based framework proposed by Bhattarai *et al.* (2011):

1. Attachment: viruses attach to soil particles with an attachment rate k_{12}
2. Movement: viruses attached to soil particles (soil + virus aggregate) are moved by surface flow velocity (u) with rate constant k_{23}
3. Detachment: viruses attached to soil particles become detached with the detachment rate k_{21}
4. Inactivation: viruses become inactivated with decaying rate k_d
5. Infiltration: viruses are removed by infiltration with the rate equal to f/D (f is saturated hydraulic conductivity, and D is flow depth).

Concentrations of free virus in water (C_1), attached to immobile soil particles (C_2), attached to mobile soil particles (C_3) were calculated using the following set of mass balance equations:

$$\frac{\partial C_1}{\partial t} + u\frac{\partial C_1}{\partial x} = -\left(k_{12} + k_d + \frac{f}{D}\right)C_1 + k_{21}C_2 \quad (1)$$

$$\frac{\partial C_2}{\partial t} = k_{12}C_1 - k_{21}C_2 - k_{23}C_2 \quad (2)$$

$$\frac{\partial C_3}{\partial t} + u\frac{\partial C_3}{\partial x} = k_{23}C_2 - \left(k_d + \frac{f}{D}\right)C_3 \quad (3)$$

where k_{12} = rate constant for the conversion of pathogen from C1 to C2 state, k_{21} = rate constant for the conversion of pathogen from C2 to C1 state, k_{23} = rate constant for the conversion of pathogen from C2 to C3 state, and k_d = virus decay rate.

The system of mass-balance equations was solved using the following initial and boundary conditions: (a) initial conditions: $C_1^0 = C_1(0, x)$; $C_2(0, x) = C_3(0, x) = 0$, where C_1^0 is the concentration of rotavirus applied to the system; and (b) boundary condition: $C_1(t, 0) = C_2(t, 0) = C_3(t, 0) = 0$. These conditions reflected the assumptions that at time zero the rotavirus particles were unattached and freely moving in the water, and no continuous source of rotavirus exists at $x = 0$.

Since viruses were immobile in the C_2 stage, the flow velocity component in Equation (2) was considered zero. However, virus concentrations in the C_1 and C_3 stages were in mobile flow and moved downstream with surface flow. In this study, the surface velocity was obtained from the Water Erosion Prediction Project (WEPP) simulation results and assumed to be constant over the space domain for each iteration. The partial differential equations (PDEs) for C_1 and C_3 have the form of a wave equation (hyperbolic PDE). Since the flow velocity (v) was assumed constant, the grid for the finite difference method could be discretized using $dx = v\ dt$ for each iteration. The system of Equations (1)–(3) was solved with the method of characteristics (Park *et al.* 2008; Bhattarai *et al.* 2011). In the presence of vegetation, an additional equation (similar to Equation (2)) was added to the model which could represent attachment to the vegetation with the rate k_{14} and detachment from the vegetation with the rate k_{41}.

Model parameter identification

The modeling framework included the coupling of a soil erosion model (WEPP), with a pathogen transport model to capture the dynamics of sediment-bound pathogens. The WEPP is a physically based erosion prediction model applicable to erosion processes on single hillslopes and small watersheds (Nearing *et al.* 1989; Cochrane & Flanagan 1999). Outputs from WEPP simulations were used as input for the pathogen transport model (Bhattarai *et al.* 2011). The WEPP model is capable of predicting soil loss and sediment deposition from the overland flow on hillslope and the concentrated flow in small channels.

For the rotavirus transport study, a 20-minute single rainfall simulation on a laboratory tilting soil bed was performed. The input for the WEPP model included: climate data including the rainfall amount and duration; hillslope profile including area, shape, and inclination of the hillslope; soil types; and cover conditions, etc. The WEPP simulations provided: (a) average flow depth and average flow rate, which can be calculated from the Chezy coefficient and the peak runoff rate; (b) average soil loss per detachment area; and (c) the soil particle fraction exiting in the flow.

For modeling purposes, microorganisms and soil particles can be considered as two substances that interact with each other producing the third constituent: microorganism-soil particle aggregates. The strength of attachment of microorganisms to soil particles depends on the chemical characteristics of soils which are highly influenced by the particle size. The mathematical representation of inter-particle interactions can be obtained experimentally or from an erosion model (suspended sediment). The particle size distribution in the suspended sediment is predicted by the WEPP model.

Initial approximation for the parameter k_{12} was obtained from a study by Ling *et al.* (2003). They conducted a long centrifuge experiment to obtain an approximate partitioning coefficient (k_d) for bacteria. They found the coefficient to be a function of the clay content in soil as:

$$k_d = A(CLAY)^B \tag{4}$$

where CLAY = the percentage of clay particles <0.002 mm in soil (the relationship was developed for $2 <$ CLAY % <50), A = the slope of the regression in log-log coordinates (101.6 ± 0.9), B = the intercept of the regression in log-log coordinates (1.98 ± 0.7).

Parameter k_{23} is the rate of microorganism-soil particle aggregate removal from the soil surface and can be obtained by analogy with soil erosion processes. Soil erosion mainly occurs due to raindrop impact and erosion caused by flowing water. Since the effect of these mechanisms is additive, initial approximation for k_{23} can be obtained as:

$$k_{23} = ad_{23}\ P + ae_{23}\ vS \tag{5}$$

where $ad_{23} = 1/D$ = detachability coefficient, P = rainfall intensity, ae_{23} = coefficient of micro-aggregate entrainment by the flow, v = flow velocity, and S = bed slope.

Both of the vegetation parameters k_{14} and k_{41} were treated as calibration parameters in the absence of reliable parameter estimates in the literature.

RESULTS AND DISCUSSION

The pathogen transport model developed by Bhattarai (2011) was combined with WEPP to predict the fate and transport kinetics of infective rotavirus particles. The model was validated using data provided by Davidson *et al.* (2016). The results are presented and discussed in the following sections.

Runoff volume and rotavirus recovery

It was observed that the volumes of surface runoff obtained from the bare-ground conditions were consistently higher than those from vegetated conditions. This was observed for all three soils and both surface cover types. These findings were expected since reduced runoff volumes from the vegetation cover were associated with more resistance to overland flow and longer contact times allowing a higher infiltration of water into the soil profile. Similarly, the rotavirus recovery also followed the same trend. More infective rotavirus particles were recovered from the bare surface condition compared to the vegetated surface conditions. In terms of bare soil beds, the highest amount of infective rotavirus particles was recovered from the bare Catlin soil and the lowest recovery was observed from the bare Alvin soil. Rotavirus recovery from the bare and vegetated Alvin soil beds was smaller compared to those from Catlin or Darwin soil beds (Davidson *et al.* 2016).

Modeling result

For the WEPP model, many input parameters were obtained from the experimental setup such as soil plot length of 0.61 m, rainfall intensity of 65 mm/hr applied for 20 minutes and three different soil types (Catlin, Darwin and Alvin). Hence, initial saturation level (antecedent moisture content) and soil hydraulic conductivity were used as the calibration parameters. The parameters were calibrated in such a way that Nash–Sutcliffe efficiency index or EI (Nash & Sutcliffe 1970) and coefficient of determination (R^2) between observed and simulated runoff rate were maximized. Since the moisture holding capacities and hydraulic concavities of bare and vegetated surfaces are different, the parameters were calibrated separately for those two conditions.

Runoff rate and volume

It was observed that WEPP simulation results for surface runoff rates were very consistent with the observed values for all three cover (bare and two vegetation types) and soil conditions. For example, the WEPP model results were in close agreement with the observed results for the Catlin soil beds with all three surface conditions (R^2 values of 0.65, 0.41 and 0.81 for bare, Brome and Fescue cover conditions, respectively). Figure 1(a) and (b) show the comparison of the experimental data with WEPP simulation

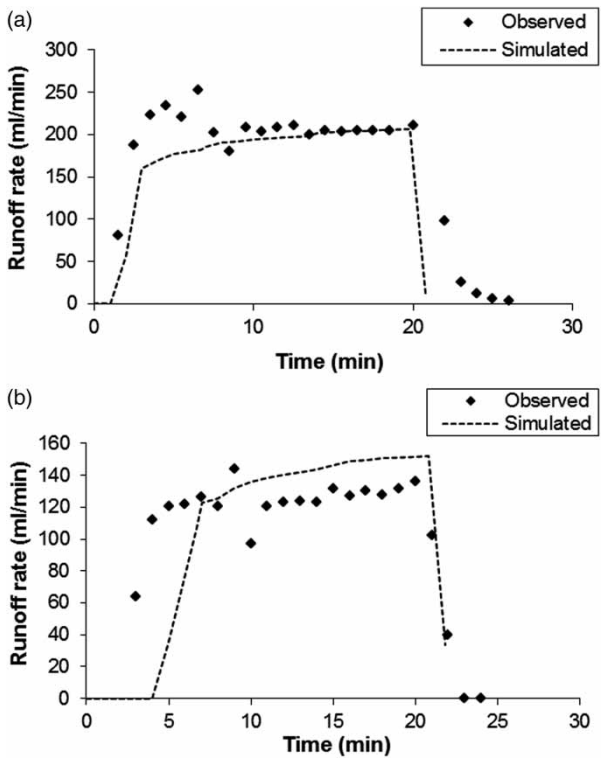

Figure 1 | Comparison of measured and WEPP simulated surface runoff values for Catlin soil bed (2.5% slope) subjected to a 65 mm/hr rainfall, applied for 20 minutes: (a) bare, (b) with Brome vegetative cover.

result for surface runoff for bare ground and Brome cover conditions for Catlin soil. Since it is not practical to present the results from all three soil types and cover conditions used for the experiments, the WEPP simulation results from representative scenarios are presented.

For Alvin soil, the WEPP model produced reasonable results for surface runoff for the bare and two vegetated conditions as compared with the observations (R^2 values of 0.62, 0.37 and 0.48 for bare, Brome and Fescue cover conditions, respectively). The comparison of simulated WEPP model results with observations for bare and Brome vegetative cover is presented in Figure 2(a) and (b).

The comparison of the experimental data with the WEPP simulation results for surface runoff from the bare ground and two vegetated conditions for Darwin also showed a good agreement (R^2 values of 0.78, 0.83 and 0.72 for values for bare, Brome and Fescue cover conditions, respectively). The observed surface runoff rate for the Darwin soil bed with Fescue vegetation was much lower than the rate for the Brome grass cover condition. The difference in factors such as root zone depth, surface cover and leaf area index between the Brome and Fescue grasses may be attributed to the decrease in surface runoff rate.

The statistical measure of goodness of fit between measured and WEPP simulated runoff rate for the three different cover and soil conditions is presented in Table 1. It was observed that both EI and R^2 values were high for the bare condition for all three soils. EI values for three vegetated cases were negative indicating the mean observed was a better estimate of the simulated results.

Figure 3 shows the comparison of simulated results from WEPP for total runoff volume with the observed values for the three surface conditions and three soil conditions. The results obtained from the WEPP simulations for total runoff volume were similar to those measured during laboratory experiments. These results indicate that the WEPP model can predict the surface runoff rate and total volume quite well for small scale laboratory experiments.

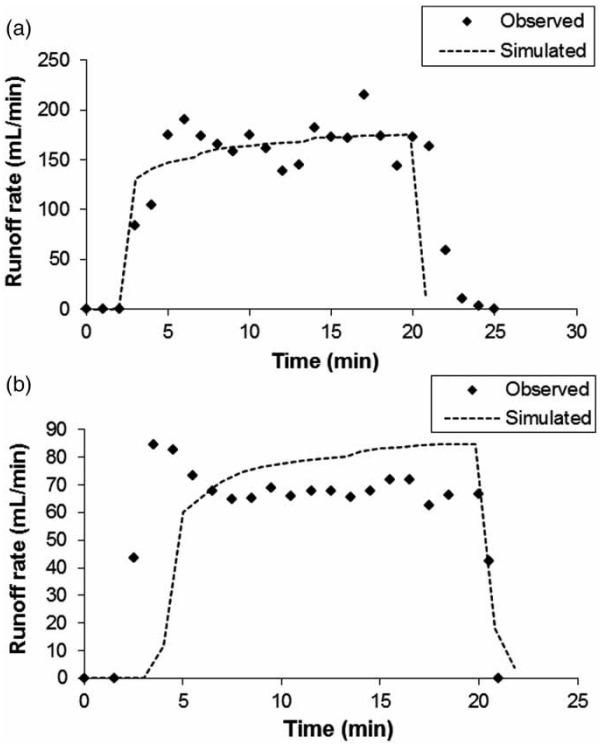

Figure 2 | Comparison of measured and WEPP simulated surface runoff values for Alvin soil bed (2.5% slope) subjected to a 65 mm/hr rainfall, applied for 20 minutes: (a) bare, (b) with Fescue vegetative cover.

Table 1 | Statistical analysis of simulated and observed runoff

Surface condition	Soil type	Nash–Sutcliffe EI	R^2
Bare	Catlin	0.93	0.65
Vegetated (Brome)	Catlin	0.86	0.41
Vegetated (Fescue)	Catlin	0.65	0.81
Bare	Darwin	0.64	0.78
Vegetated (Brome)	Darwin	0.71	0.83
Vegetated (Fescue)	Darwin	−4.27	0.72
Bare	Alvin	0.56	0.62
Vegetated (Brome)	Alvin	−0.63	0.37
Vegetated (Fescue)	Alvin	−0.12	0.48

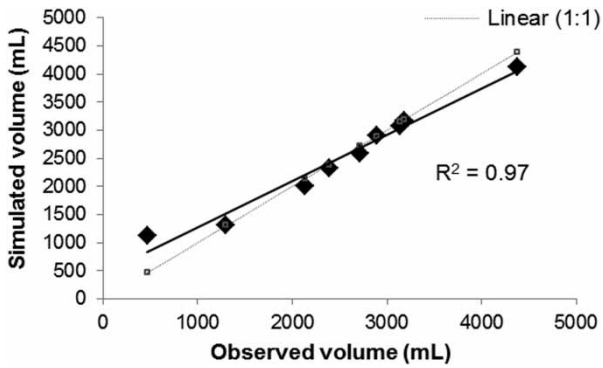

Figure 3 | Comparison of WEPP simulation results with observations for surface runoff volume for different cover and soil conditions.

Rotavirus recovery

After calibrating the WEPP model, the simulated outputs were used to drive the pathogen transport model. The WEPP model simulations provided the input parameters: bed slope, rainfall intensity, flow velocity, flow depth, saturated hydraulic conductivity and soil loss for the rotavirus transport model. During the calibration process, the break-through curve from the rotavirus transport model was compared with the laboratory experiments to estimate different attachment factors k_{12}, k_{23}, k_{21} for bare soil and additionally k_{14} and k_{14} for vegetated conditions.

The rotavirus break-through curve in surface runoff observed during the experiments and obtained from the pathogen transport model simulations for all three cover conditions and three soil types were compared. Comparison of observed and simulated break-through curves for bare and vegetated (Brome and Fescue grasses) Catlin soil beds revealed that the rotavirus transport model produced reasonable results (R^2 values of 0.60, 0.77 and 0.71 for bare, Brome, and Fescue cover conditions, respectively). Figure 4(a) and (b) show the comparison of break-through curves obtained from the rotavirus transport model with experimental data for Catlin soil beds with bare and Brome covers. Since three soil types and cover conditions were used for the experiments, comparison of model simulation results with observed break-through curve for selected cases are presented. The model could reproduce the first peak observed during the experiment but the recovery pattern was slightly different from the observations for subsequent peaks. As seen in Figure 4(b), experimental results showed a small increase in infective rotavirus particle recovery around 16 minutes and the model simulation could not capture this increase. Even though the simulated results matched the very first peak observed during experiments in most cases, the model could not reproduce multiple peaks obtained from experimental results and under-predicted total rotavirus recovery in other similar cases.

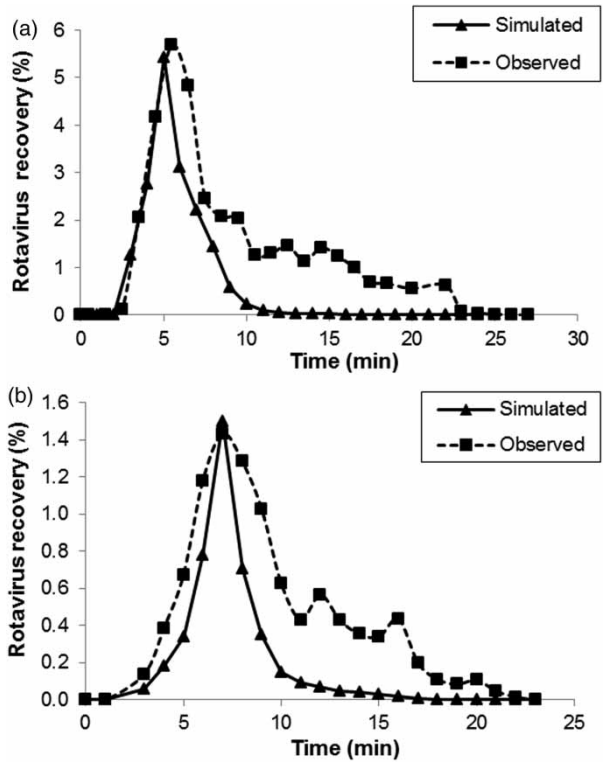

Figure 4 | Rotavirus transport in surface runoff for Catlin soil bed (2.5% slope) under a 65 mm/hr rainfall, applied for 20 minutes (a) bare (b) with Brome grass vegetation cover.

The comparison of observed data with the rotavirus transport model simulation results for surface runoff for bare ground and the two vegetated (Brome and Fescue grasses) conditions for Alvin soil indicated that the rotavirus transport model produced reasonable results (Figure 5(a) and (b)). For bare and Fescue cover conditions, there was a very good match between the observed and simulated results (R^2 values of 0.98 and 0.92 respectively). In the case of the Brome grass cover condition, the observed break-through curve showed multiple peaks. The rotavirus transport model could only replicate the timing and amount of recovered rotavirus particles in the observed first peak but not the other peaks. Hence, the computed R^2 value between observed and simulated rotavirus recovery was lower (0.77) in the case of Brome grass cover condition compared to bare or Fescue cover.

For Alvin soil, the experimental data showed more than one peak in the rotavirus break-through curve for all three cover (bare and two vegetated) conditions. The rotavirus transport model could reproduce the first peak seen during the experiments; it could not replicate remaining peaks. Hence, the comparison of observation and model simulation resulted in low R^2 values (0.61 for bare and 0.26 for Brome cover conditions).

Figure 6 shows the comparison of total rotavirus recovery obtained from the transport model with the experimental results for three soils and three cover

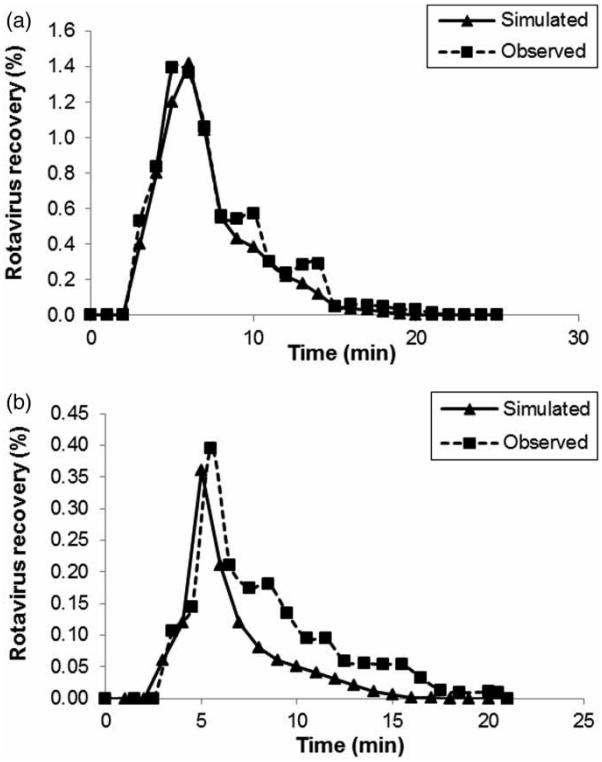

Figure 5 | Rotavirus transport in surface runoff for Alvin soil bed (2.5% slope) under a 65 mm/hr rainfall, applied for 20 minutes: (a) bare, (b) with Fescue vegetative cover.

conditions. The simulated results showed that the percent recovery was higher for Catlin and Darwin soils compared to Alvin soil which also confirms the findings from experimental results. Although the comparison graph indicates a high value of R^2 (0.93), the model simulation underestimated rotavirus recovery in the cases when multiple peaks were observed during experiments.

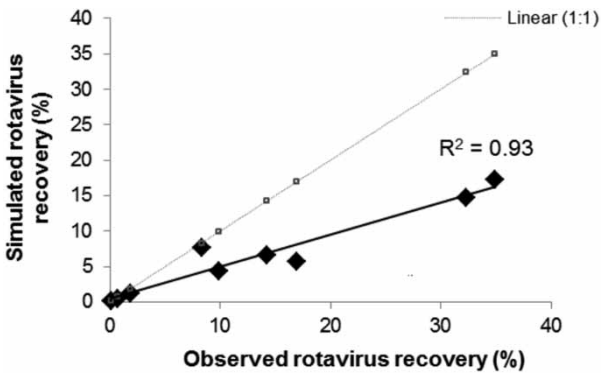

Figure 6 | Comparison of simulated and observed results for rotavirus recovery for different cover and soil conditions.

Although the relation provided by Ling *et al.* (2003) gave an initial parameter to drive the model for bare soil conditions, the one parameter approach for all soil and cover conditions did not produce satisfactory results in many cases. In the absence of an alternative reliable approach that can incorporate various soil and cover types in a partitioning coefficient, the parameters k_{12} had to be calibrated for each case by comparing model results with the experimental data. The different values of attachment and detachment rate parameters (k_{12}, k_{23}, k_{21} for bare soil and additionally k_{14} and k_{14} for vegetated condition) had to be used during simulation process to replicate the result obtained from the experiments.

Table 2 shows calibrated rotavirus partition coefficients for bare and vegetated surface conditions for Alvin, Catlin and Darwin soils. It was observed that the parameters k_{12} and k_{21} were more sensitive compared to the parameter k_{23}. The parameter k_{12} affected the peak of the rotavirus recovery curve while the parameter k_{21} dictated the shape of the curve. Parameter k_{23} governed the formation of pathogen and soil particle aggregate which was not quantified in this study. In the case of vegetated surface, parameters k_{12} and k_{14} were two sensitive parameters, which governed how many pathogens got attached to soil surface and vegetation, respectively. Parameters k_{21} and k_{41} were another set of

Table 2 | Calibrated model coefficients for different cover conditions and soil types for rotavirus

Soil type	Cover condition	Parameters				
		k_{12}	k_{21}	k_{23}	k_{14}	k_{41}
Alvin	Bare	0.201	0.136	0.05		
	Vegetated (Brome)	0.341	0.046	0.05	0.314	0.084
	Vegetated (Fescue)	0.229	0.131	0.05	0.208	0.116
Catlin	Bare	0.154	0.184	0.05		
	Vegetated (Brome)	0.228	0.128	0.05	0.156	0.085
	Vegetated (Fescue)	0.236	0.089	0.05	0.186	0.098
Darwin	Bare	0.161	0.178	0.05		
	Vegetated (Brome)	0.245	0.081	0.05	0.189	0.092
	Vegetated (Fescue)	0.342	0.042	0.05	0.315	0.091

sensitive parameters which governed how many pathogens got released from soil surface and vegetation, respectively.

These simulated results indicated that one partitioning parameter based on soil clay content as used by Ling *et al.* (2003) might not be valid for rotavirus and similar microorganisms for varying environmental and topographic conditions. Future modeling attempts must include the dynamic nature of environmental and topographic condition for formulating the partitioning parameters.

CONCLUSIONS

A physically based approach for modeling rotavirus fate and transport in surface flow has been presented. Deterministic descriptions of the processes have been employed and a correspondence between them has been established and model parameters have been identified from the literature. Another feature of the model is the incorporation of an erosion model (WEPP) into the microorganism transport model, thereby establishing a link between the sediment and microbial transport, and highlighting the capability of the suspended sediment to transport microbes in the overland flow. Model results were compared with small-scale experimental data and the model performed well in most cases. Although the model replicated the kinetics of infective rotavirus recovery from surface runoff, the model under-predicted recovery when experimental data showed multiple peaks in the rotavirus break-through curve. The under-prediction in simulated results can be attributed to simplification of complex processes and model parameter uncertainty. The model results can be improved by training the model with more data which will help reduce model and parameter uncertainty.

REFERENCES

Atwill, E. R., Hou, L., Karle, B. M., Harter, T., Tate, K. W. & Dahlgren, R. A. 2002 Transport of *Cryptosporidium parvum* oocysts through vegetated buffer strips and estimated filtration efficiency. *Appl. Environ. Microbiol.* **68**, 5517–5527.

Bhattarai, R. 2011 Modeling Fate and Transport of *Cryptosporidium parvum* and Rotavirus in Overland Flow. Doctoral Dissertation. Department of Agricultural and Biological Engineering, University of Illinois at Urbana-Champaign.

Bhattarai, R., Kalita, P., Trask, J. & Kuhlenschmidt, M. S. 2011 Development of a physically-based model for transport of *Cryptosporidium parvum* in overland flow. *Environ. Model. Softw.* **26**, 1289–1297.

Canale, R., Auer, M., Owens, E., Heidtke, T. & Effler, S. 1993 Modelling fecal coliform bacteria II. Model development and application. *Water Res.* **27**, 703–714.

Chu, Y., Jin, Y., Baumann, T. & Yates, M. V. 2003 Effect of soil properties on saturated and unsaturated virus transport through columns. *J. Environ. Qual.* **32**, 2017–2025.

Cochrane, T. A. & Flanagan, D. C. 1999 Assessing water erosion in small watersheds using WEPP with GIS and digital elevation models. *J. Soil Water Conserv.* **54**, 678–685.

Conner, M. E. & Darlington, R. W. 1980 Rotavirus infection in foals. *Am. J. Vet. Res.* **41**, 1699–1703.

Conner, M. E., Estes, M. K. & Graham, D. Y. 1988 Rabbit model of rotavirus infection. *J. Virol.* **62**, 1625–1633.

Davidson, P. C., Kuhlenschmidt, T. B., Bhattarai, R., Kalita, P. K. & Kuhlenschmidt, M. S. 2013 Investigation of rotavirus survival in different soil fractions and temperature conditions. *J. Environ. Protect.* **4**, 1–9.

Davidson, P. C., Kuhlenschmidt, T. B., Bhattarai, R., Kalita, P. K. & Kuhlenschmidt, M. S. 2014 Effects of soil type and cover condition on *Cryptosporidium parvum* transport in overland flow. *Water Air Soil Pollut.* **225**, 1882.

Davidson, P. C., Kuhlenschmidt, T. B., Bhattarai, R., Kalita, P. K. & Kuhlenschmidt, M. S. 2016 Overland transport of rotavirus and the effect of soil type and vegetation. *Water* **8** (3), 78.

Dorner, S. M., Anderson, W. B., Slawson, R. M., Kouwen, N. & Huck, P. M. 2006 Hydrologic modeling of pathogen fate and transport. *Environ. Sci. Technol.* **40**, 4746–4753.

Feng, N., Lawton, J. A., Gilbert, J., Kuklin, N., Vo, P., Prasad, B. V. V. & Greenberg, H. B. 2002 Inhibition of rotavirus replication by a non-neutralizing, rotavirus VP6–specific IgA mAb. *J. Clin. Invest.* **109**, 1203–1213.

Ferrari, M. & Gualandi, G. L. 1986 A serologic survey of rotavirus infection in pigs. *Microbiologica* **9**, 29–32.

Fischer, T. K., Viboud, C., Parashar, U., Malek, M., Steiner, C., Glass, R. & Simonsen, L. 2007 Hospitalizations and deaths from diarrhea and rotavirus among children <5 years of age in the United States, 1993–2003. *J. Infect. Dis.* **195**, 1117–1125.

Fraser, R., Barten, P. & Pinney, D. 1998 Predicting stream pathogen loading from livestock using a geographical information systems-based delivery model. *J. Environ. Qual.* **27**, 935–945.

Gagliardi, J. V. & Karns, J. S. 2000 Leaching of *Escherichia coli* o157:H7 in diverse soils under various agricultural management practices. *Appl. Environ. Microbiol.* **66**, 877–883.

Gotkowitz, M. B., Bradbury, K. R., Borchardt, M. A., Zhu, J. & Spencer, S. K. 2016 Effects of climate and sewer condition on virus transport to groundwater. *Environ. Sci. Technol.* **50**, 8497–8504.

Harter, T., Wagner, S. & Atwill, E. R. 2000 Colloid transport and filtration of *Cryptosporidium parvum* in sandy soils and aquifer sediments. *Environ. Sci. Technol.* **34**, 62–70.

Jamieson, R. C., Gordon, R. J., Sharples, K. E., Stratton, G. W. & Madani, A. 2002 Movement and persistence of fecal bacteria in agricultural soils and subsurface drainage water: a review. *Can. Biosyst. Eng.* **44**, 11–19.

Jamieson, R., Gordon, R., Joy, D. & Lee, H. 2004 Assessing microbial pollution of rural surface waters: a review of current watershed scale modeling approaches. *Agric. Water Manage.* **70**, 1–17.

Koch, D. J., Davidson, P. C., Kalita, P. K., Kuhlenschmidt, M. S. & Kuhlenshmidt, T. B. 2013 Fate and transport of *Cryptosporidium parvum* under small-scale rainfall simulator. *J. Med. Res. Dev.* **2**, 93–100.

Liao, H., Krometis, L. A. H. & Kline, K. 2016 Coupling a continuous watershed-scale microbial fate and transport model with a stochastic dose-response model to estimate risk of illness in an urban watershed. *Sci. Total Environ.* **551**, 668–675.

Ling, T. Y., Achberger, E. C., Drapcho, C. M. & Bengtso, R. L. 2003 Quantifying adsorption of an indicator bacteria in a soilwater system. *Trans. ASAE* **45**, 669–674.

McLaughlin, S. J., Kalita, P. K. & Kuhlenschmidt, M. S. 2013 Fate of *Cryptosporidium parvum* oocsyts within soil, water, and plant environment. *J. Environ. Manage.* **131**, 121–128.

McMurry, S. W., Coyne, M. S. & Perfect, E. 1998 Fecal Coliform transport through intact soil blocks amended with poultry manure. *J. Environ. Qual.* **27**, 86–92.

Moore, J. A., Smyth, J. D., Baker, E. S., Miner, J. R. & Moffitt, D. C. 1989 Modeling bacteria movement in livestock manure systems. *Trans. ASAE* **32**, 1049–1053.

Nash, J. E. & Sutcliffe, J. V. 1970 River flow forecasting through conceptual models part I – A discussion of principles. *J. Hydrol.* **10**, 282–290.

Nearing, M. A., Foster, G. R., Lane, L. J. & Finkner, S. C. 1989 A process based soil erosion model for USDA-water erosion prediction project technology. *Trans. ASAE* **32**, 1587–1593.

Niazi, M., Obropta, C. & Miskewitz, R. 2015 Pathogen transport and fate modeling in the Upper Salem River watershed using SWAT model. *J. Environ. Manage.* **151**, 167–177.

Ojha, C., Surampalli, R., Sharma, P. & Joshi, N. 2011 Breakthrough curves and simulation of virus transport through fractured porous media. *J. Environ. Eng.* **137**, 731–739.

Pachepsky, Y. A., Sadeghi, A. M., Bradford, S. A., Shelton, D. R., Guber, A. K. & Dao, T. H. 2006 Transport and fate of manure-borne pathogens: modeling perspective. *Agric. Water Manage.* **86**, 81–92.

Pandey, P. K., Soupir, M. L., Ikenberry, C. D. & Rehmann, C. R. 2016 Predicting streambed sediment and water column Escherichia coli levels at watershed scale. *JAWRA J. Am. Water Resour. Assoc.* **52**, 184–197.

Parajuli, P. B., Mankin, K. R. & Barnes, P. L. 2009 Source specific fecal bacteria modeling using soil and water assessment tool model. *Bioresour. Technol.* **100**, 953–963.

Park, Y., Yeghiazarian, L., Stedinger, J. R. & Montemagno, C. D. 2008 Numerical approach to Cryptosporidium risk assessment using reliability method. *Stoch. Environ. Res. Risk Assess.* **22**, 169–183.

Passmore, J. M., Rudolph, D. L., Mesquita, M. M. F., Cey, E. & Emelko, M. B. 2010 The utility of microspheres as surrogates for the transport of E. coli RS2 g in partially saturated agricultural soil. *Water Res.* **44**, 1235–1245.

Powelson, D. K., Simpson, J. R. & Gerba, C. P. 1990 Virus transport and survival in saturated and unsaturated flow through soil columns. *J. Environ. Qual.* **19**, 396–401.

Rolsma, M. D., Kuhlenschmidt, T. B., Gelberg, H. B. & Kuhlenschmidt, M. S. 1998 Structure and function of a ganglioside receptor for porcine rotavirus. *J. Virol.* **72**, 9079–9091.

Sadeghi, A. & Arnold, J. 2002 A SWAT/Microbial sub-model for predicting pathogen loadings in surface and groundwater at watershed and basin scales. In: *Proceedings of Total Maximum Daily Load (TMDL) Environmental Regulations Conference*. Fort Worth, Texas, pp. 56–63.

Sim, Y. & Chrysikopoulos, C. V. 2000 Virus transport in unsaturated porous media. *Water Resour. Res.* **36**, 173–179.

Smith, M. & Tzipori, S. 1979 Gel electrophoresis of rotavirus RNA derived from six different animal species. *Aust. J. Exp. Biol. Med. Sci.* **57**, 583–585.

Smith, M. S., Thomas, G. W., White, R. E. & Ritonga, D. 1985 Transport of *Escherichia coli* through intact and disturbed soil columns. *J. Environ. Qual.* **14**, 87–91.

Tate, K. W., Pereira, M. D. & Atwill, E. R. 2004 Efficacy of vegetated buffer strip for *Cryptosporidium parvum*. *J. Environ. Qual.* **33**, 2243–2251.

Tian, Y., Gong, P., Radke, J. & Scarborough, J. 2002 Spatial and temporal modeling of microbial contaminants on grazing farmland. *J. Environ. Qual.* **31**, 860–869.

Trask, J. R., Kalita, P. K., Kuhlenschmidt, M. S., Smith, R. D. & Funk, T. L. 2004 Overland and near-surface transport of *Cryptosporidium parvum* from vegetated and nonvegetated surfaces. *J. Environ. Qual.* **33**, 984–993.

Walker, F. R. & Stedinger, J. R. 1999 Fate and transport model of Cryptosporidium. *J. Environ. Eng.* **125**, 325–333.

Walker, S. E., Mostaghimi, S., Dillaha, T. & Woeste, F. 1990 Modeling animal waste management practices: impacts on bacteria levels in runoff from agricultural lands. *Trans. ASAE* **33**, 807–817.

Wilkinson, J., Jenkins, A., Wyer, M. & Kay, D. 1995 Modelling faecal coliform dynamics in streams and rivers. *Water Res.* **29**, 847–855.

Wray, C., Dawson, M., Afshar, A. & Lucas, M. 1981 Experimental *Escherichia coli* and rotavirus infection in lambs. *Res. Vet. Sci.* **30**, 379–381.

Yeghiazarian, L. L., Walker, M. J., Binning, P., Parlange, J. Y. & Montemagno, C. D. 2006 A combined microscopic and macroscopic approach to modeling the transport of pathogenic microorganisms from nonpoint sources of pollution. *Water Resour. Res.* **42**, W09406.

First received 22 August 2016; accepted in revised form 26 April 2017. Available online 25 May 2017